Int J Adv Manuf Technol (2015) 76:1215–1224
DOI 10.1007/s00170-014-6373-7

ORIGINAL ARTICLE

Dynamic error budget analysis of an ultraprecision flycutting machine tool

Yazhou Sun · Wanqun Chen · Yingchun Liang · Chenhui An · Guoda Chen · Hao Su

Received: 1 May 2014 / Accepted: 8 September 2014 / Published online: 16 September 2014

Abstract This paper presents an error budget methodology for designing and characterizing machines used to manufacture or inspect parts with spatial frequency-based specifications. In this methodology, the static and dynamic error are considered in the error budget; the static error affects the figure accuracy, while the dynamic error introduces the spatial frequency domain error. The error caused by the components of the machine tool, the cutting process and the external interference, are considered in this paper. Using the error budget, it is able to minimize risk during initial stages by ensuring that the machine will produce components that meet specifications before the machine is actually built or purchased. This methodology is used to predict and improve the performance of an ultraprecision flycutting machine tool.

Keywords Error budget · Spatial frequency domain · Dynamics · Ultraprecision · Machine design

1 Introduction

The spatial frequency-based specifications (SFBS) are very important for the advanced optical and weapon system, such as the potassium dihydrogen phosphate (KDP) crystal and neodymium glass use in National Ignition Facility Project [1, 2], and optical lenses use in space telescope system [3]. In the previous experiments, the damage caused by the unsatisfied spatial frequency specifications (SFS) of the optical elements is found; Fig. 1b–e shows the damage of KDP crystal based on the experimental observation; they are front surface damage, body damage, back surface damage, and the focused beam, respectively. Figure 1f shows the self-focus in fused silica wedge. The reasons for this phenomenon are the laser self-focusing effect and waviness modulation, which are caused by the spatial frequency error in the machined surface [4, 5].

The performances of the machining equipment determine the SFS of the machined surface directly. Therefore, when designing such kind of machine tool, the spatial frequency domain error budget must be carried out. Error budgets provide the formalism whereby the designer account for all sources of uncertainty in a process and sum them to arrive at a net prediction to predict whether a manufactured component can meet a target specification. By using the error budget, the designers can minimize risk during initial stages by ensuring that the machine equipment will produce components that meet the required specifications before the machine is actually built or purchased.

Donaldson used error budget to design the Large Optics Diamond Turning Machine tolerance firstly [6]. In addition, Slocum has done much work on the geometric aspects of error budgeting using homogeneous transformation matrices [7]. Treib and Matthias used the error budget method to calculate and optimize the volumetric error field of a multiaxis system [8]. Walter et al. described how an error budget can be used as a design tool to enhance the performance of an ultraprecision diamond turning lathe, by understanding error sources and their effects on the form of a workpiece [9]. Gouws defined the error budgeting approach alongside the pure top-down and pure bottom-up approaches for control system design [10]. Hii et al. compared two design concepts of a precision electro discharge micromilling machine by the error budgeting approach [11].

Y. Sun · W. Chen (✉) · Y. Liang · G. Chen · H. Su
Center for Precision Engineering, Harbin Institute of Technology, Harbin 150001, People's Republic of China
e-mail: chwq@hit.edu.cn

C. An
Chengdu Fine Optic Engineering Research Center, Chengdu 610040, People's Republic of China

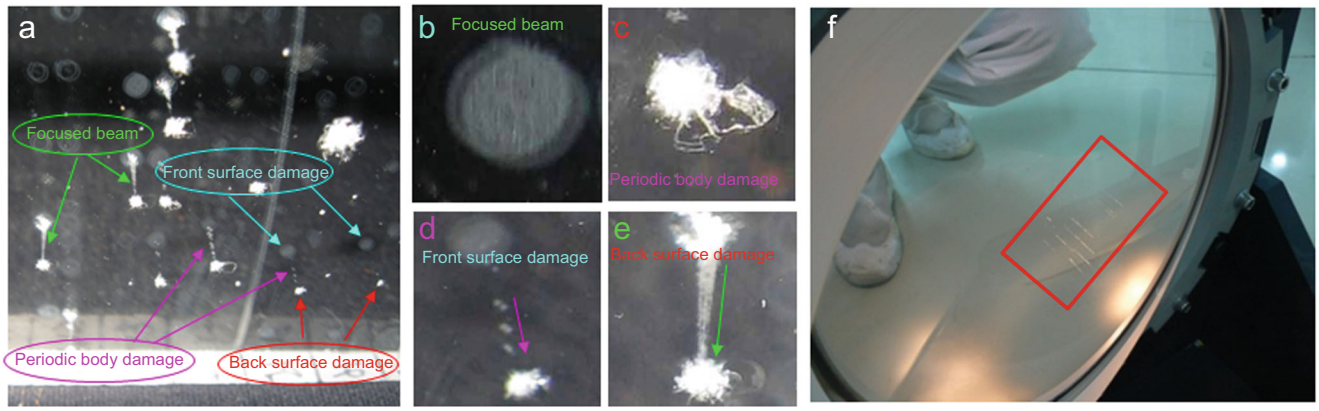

Fig. 1 Damage of optical elements during experiment: **a** the damaged surface of KDP crystal, **b** front surface damage, **c** back surface damage, **d** periodic body damage, **e** focused beam, and **f** the self-focus in fused silica wedge

However, the current error budgeting procedure aims to obtain a single number estimating the net worst case or root-mean-square (RMS) error on the workpiece. This procedure has limited ability to differentiate between low-spatial-frequency form errors versus high-frequency surface finish errors, which provides no formal mechanism for designing machines that can produce parts with SFBS [12]. In this paper, the spatial frequency domain error budget of an ultraprecision flycutting machine tool use for KDP crystal machining is presented, which can be used to budget the continuous spatial frequency content of error of this machine tool. In order to product the optical components that satisfy the SFBS, the dynamic characteristics of the machine structure, oil supply system, and cutting parameters as well as the machine components and how they interact as a system to a precision machine tool have been considered.

2 Spatial frequency domain error budget method

Figure 2 shows flowcharts for the dynamic error budget method. The first step of the dynamic error budget is to identify the physical influences that generate the dimensional errors that propagate through the machine tool. These errors include the effects such as dynamic response of the machine structure, spindle motion error, oil source fluctuations, and way non-straightness. The next step is to calculate the influence of the sources on the machining performance. A coupling mechanism that converts these physical influences into a displacement in frequency domain is given by the FE method and numerical method. The output from this procedure is the error in spatial frequency domain. Then, this number is compared to the required specifications; if the prediction meets target specifications, then the machine tool can be used to machine the required optical parts. If the prediction does not meet specifications, then the machine tool should be improved by observing which sources are the dominating contributing errors.

3 Spatial frequency domain error budget of a flycutting machine

The KDP crystal mainly functions as harmonic frequency converters in modern high-energy solid-state lasers, polarization rotators in Pockels cells, and laser fusion system in the inertial confinement fusion (ICF) program, owning to its good nonlinear optical and electro-optical properties [13, 14]. In order to meet the optical requirements and reduce the laser damage threshold of the KDP crystal, the KDP crystal has extremely harsh requirements of the topography in spatial

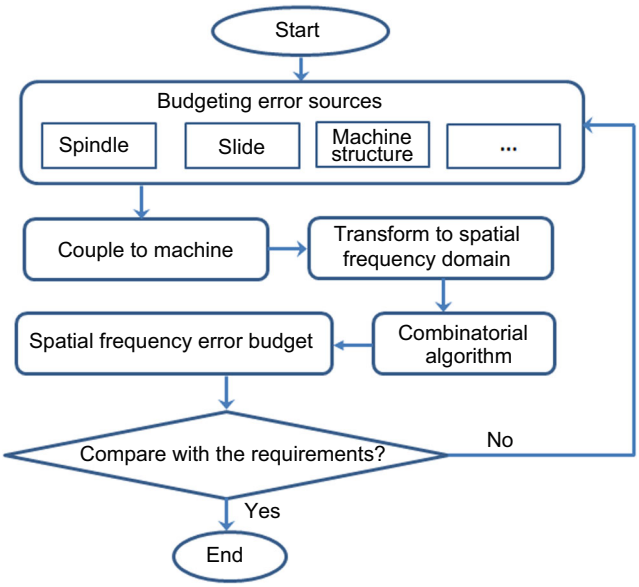

Fig. 2 Flowcharts for the dynamic error budget method

frequency domain. The specifications of the machined surface are as follows [15]:

Specification 1: Roughness values (Ra) less than 3 nm in 0.01~0.12 mm;
Specification 2: RMS no more than 4.2 nm and PSD2 better than 15 $nm^2 \cdot mm$ in 0.12~2.5 mm;
Specification 3: RMS less than 6.4 nm and PSD1 better than 15 $nm^2 \cdot mm$ in 2.5~33 mm;
Specification 4: Gradient root mean square (GRMS) better than 11 nm/cm, in the range over 33 mm.
Specification 5: Flatness less than 3 μm in 415 mm.

The flycutting machine tool used for KDP crystal machining is shown in Fig. 3; the configuration of the flycutting machine tool adopt a gantry structure. A vertical axis aerostatic spindle with flycutter over a horizontal axis hydrostatic slide is supported by a bridge. Mounted to the horizontal slide is a vacuum chuck that clamps the workpiece.

The error in the machining process mainly contains the spindle error, the slide error, the dynamic error of the machine structure, and other errors caused by the cutting process.

In order to judge whether this machine tool can be used to product the KDP crystal and how to improve the performance of the machine tool, the spatial frequency domain error budget is used as a sensitivity analysis tool to ensure that the optical parts manufactured by a machine will meet the specified component tolerances.

3.1 The errors of the aerostatic spindle

The rotation accuracy of spindle is the main factor influencing the machining accuracy of ultraprecision machine tool. The machine tool has an aerostatic spindle with a DC brushless motor. The axial and radial error motions of the spindle are tested by the spindle error analyzer (Lion Precision, Automated Quality Technologies, USA) with two precision balls and capacitance gages as shown in Fig. 4.

Figure 5 shows the accuracy of spindle under quasistatic condition; it can be found that the synchronization error and asynchronous error in axial direction is 83 and 41 nm, respectively (Fig. 6). The synchronization error and asynchronous error in radial direction are 222 and 50 nm, respectively, and from the synchronization error, 12-frequency-multiplication component can be found, which corresponding to the numbers of the orifice in the radial bearing.

The error of the spindle will differ between the quasistatic and high-speed rotation. In order to study the spindle error in work speed, the test was carried out with the rotation speed of 300 rpm. The synchronization error and asynchronous error in axial direction are 61.1 and 33.1 nm. The synchronization error and asynchronous error in radial direction are 90.8 and 35.2 nm. It can be noted that under the work speed, the motion error is decreased both in axial and radial directions, and the 12-frequency-multiplication component disappeared, which indicate that the effect of the orifice has been decreased owning to the dynamic pressure effect.

The axial error occurred in the sensitive direction of the machining process, which has important influence on machining result. Transfering the test result of the axial error from time domain to frequency domain (Fig. 7), two obvious frequency components are found in 0.98 and 6.5 Hz; the amplitude is 2.5 and 7.6 nm, respectively, which is caused by gyroscopic effect and the rotation speed, respectively. They belong to the low-frequency domain and will affect the profile accuracy.

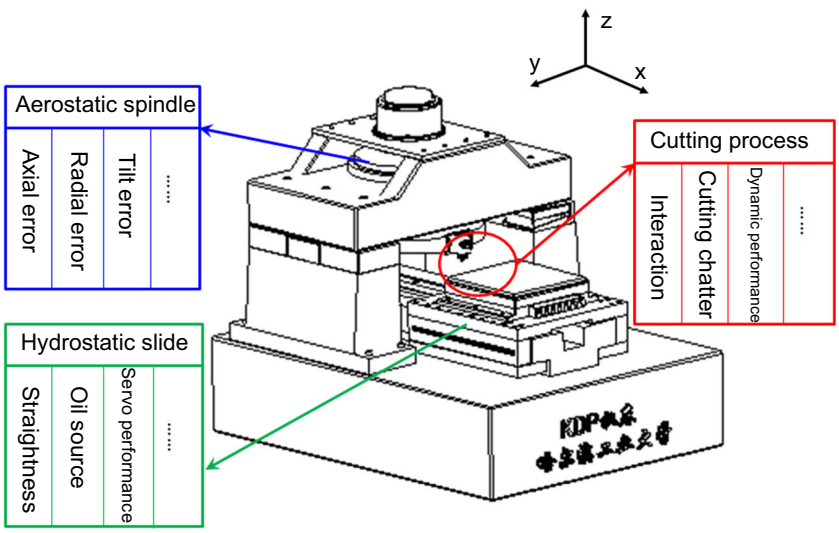

Fig. 3 Schematic diagram of the machine tool

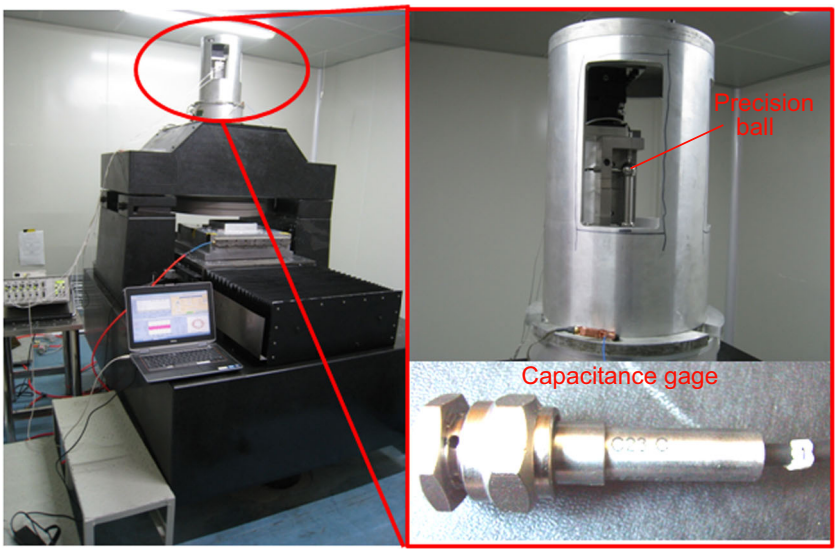

Fig. 4 The experiment of spindle error

3.2 The main errors of the hydrostatic slide

In order to improve the stiffness of the slide, the hydrostatic bearing is used in the slide. The hydrostatic slide system consists of the rail, hydrostatic bearing, worktable, and the oil supply system. The horizontal straightness of the *x*-axis was measured by the photoelectric autocollimator. Measured result shows that the straightness of the *x*-axis is less than

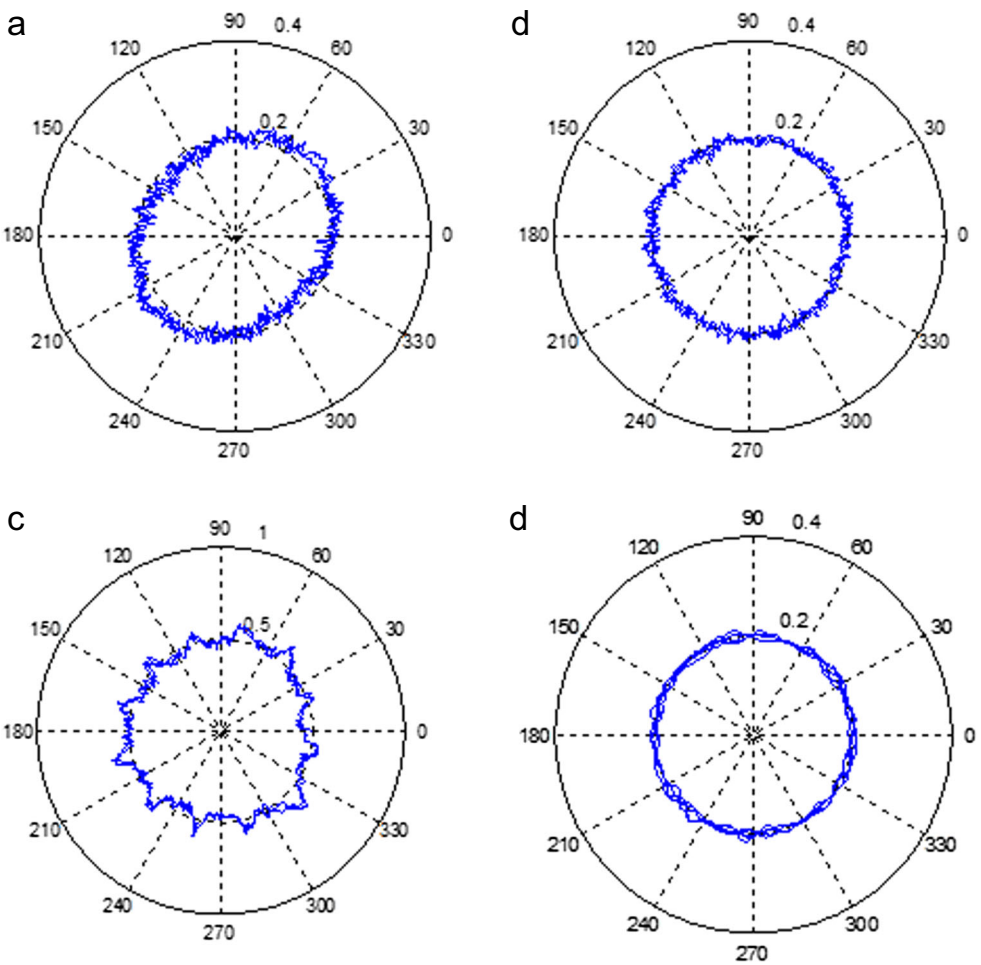

Fig. 5 The error of the spindle under quasistatic condition. **a** Synchronization error in axial direction, **b** asynchronous error in axial direction, **c** synchronization error in radial direction, **d** asynchronous error in radial direction

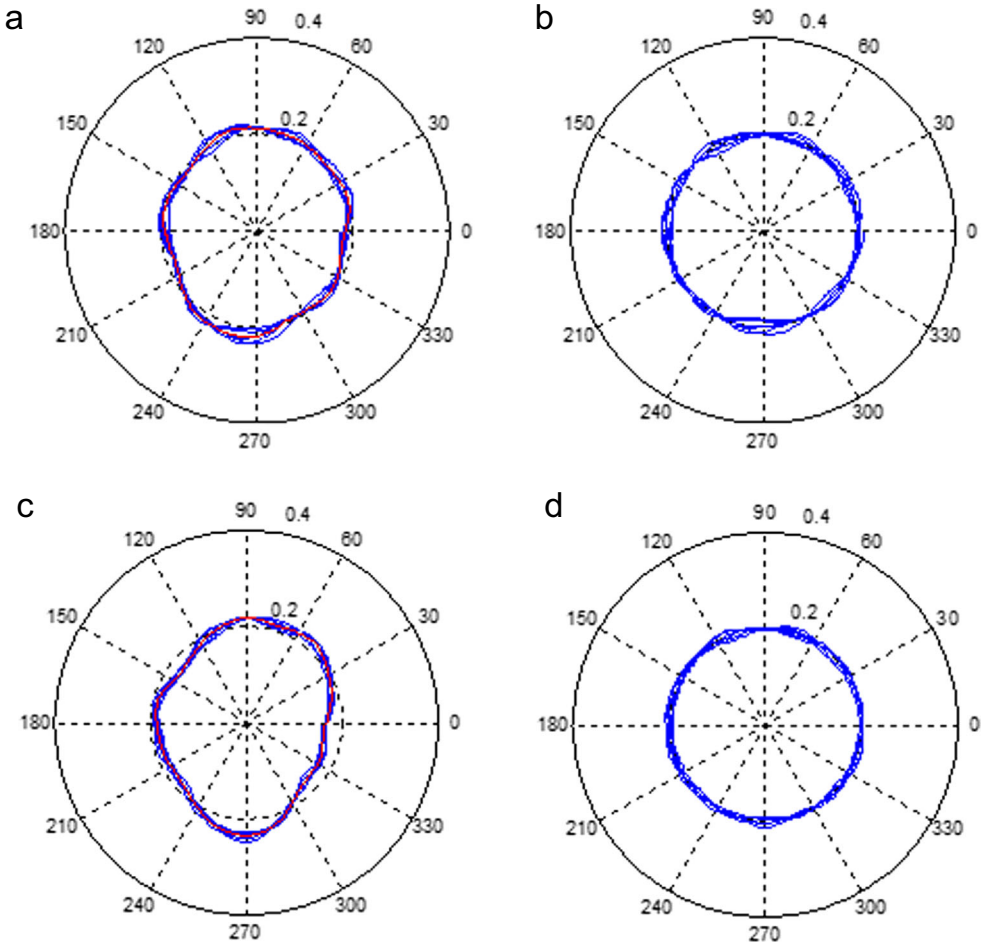

Fig. 6 The error of the spindle with work speed. **a** Synchronization error in axial direction, **b** asynchronous error in axial direction, **c** synchronization error in radial direction, **d** asynchronous error in radial direction

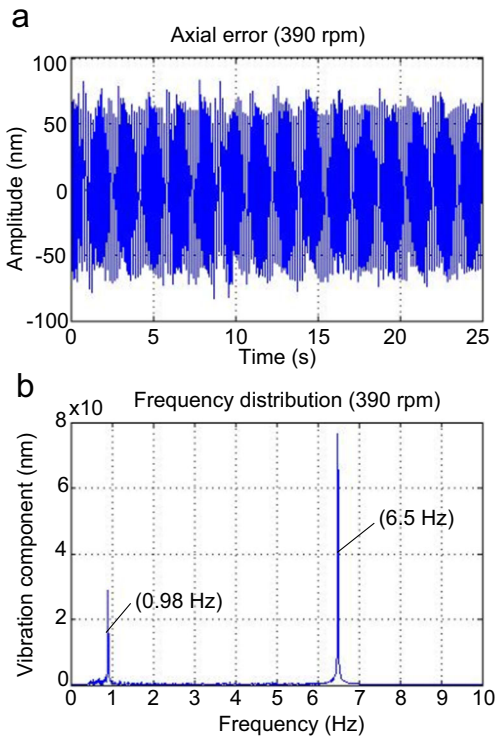

Fig. 7 The frequency domain analysis of the axial error

0.14 μm as shown in Fig. 8. The straightness of the slide belongs to the low-frequency error, which mainly affect the profile accuracy. In the hydrostatic slide system, the constant pressure oil source fluctuations will introduce the displacement error of worktable; the error occurred in the sensitive direction; therefore, it must be considered in the error budget.

The test results of the pressure fluctuations of the oil source and the displacement of the worktable caused by it are shown in Fig. 9. From Fig. 9a, it can be noted that though a constant pressure of 0.42 MPa is set for the hydraulic oil supply system, the oil source pressure fluctuations up to several KPa, which is caused by the mechanical structure of the oil supply system. According to the hydrostatic principle, the relationship between the pressure fluctuations and the slide displacement can be obtained in Fig. 9b. It can be found that the displacement of the slide is around 10 nm. The period of fluctuations of the displacement is the same as the oil source pressure fluctuations. From the PSD analysis result shown in Fig. 9c, it can be found that the waviness caused by the pressure fluctuations of the oil source mainly gathered in 0.6–1.4 mm, it belongs to the midfrequency error [16], which will affect the PSD2

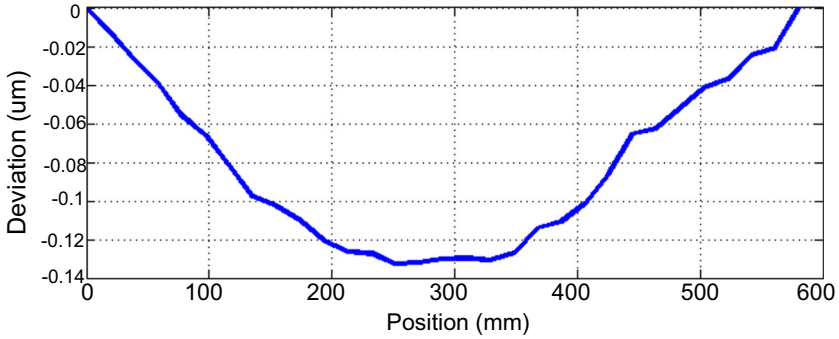

Fig. 8 The straightness of the slide

specification. The detail for the influence of oil source fluctuations on the machined result can be found in Chen et al.

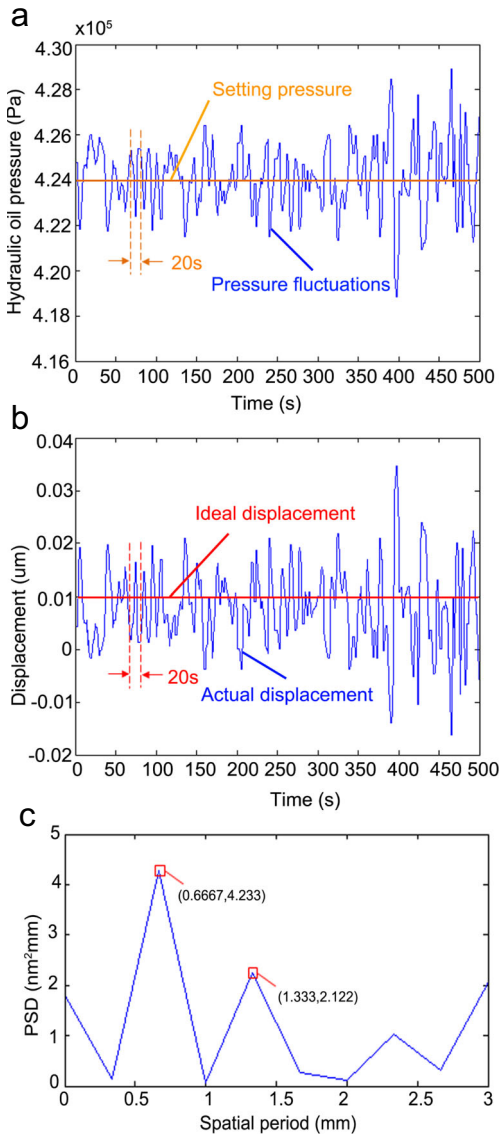

Fig. 9 Pressure fluctuations of the oil source analysis. **a** Test results of the pressure fluctuations of the oil, **b** Slide displacement under the pressure fluctuations, and **c** the frequency domain analysis

3.3 Errors caused by the machine structure

The dynamic error caused by the machine tool structure is a very important error in ultraprecision machining; it cannot be neglected in the error budget. The dynamic performance of the machine tool structure is obtained as shown in Fig. 10a by FE method; the detail of the FE model of the machine tool can be found in Liang et al. Figure 10b shows the dynamic response of the tool cutter; it can be found that under the cutting force, the cutter will generate some waviness in the machined surface [17–19]. Transfering the waviness to frequency domain, it can be noted that the waviness mainly contain three frequency 170, 192, and 336 Hz, which corresponds to the 1st, 2nd, and 4th order natural frequency of the machine structure, respectively.

The relationship between the wavelength of the waviness and the vibration frequency of the machine tool can be described as [20]

$$T_D = \frac{\pi d \times n_0 \times \cos\theta}{60\omega_n} \tag{1}$$

where d denotes the diameter of the flyhead (d=630 mm), n_0 denotes the speed of spindle, θ denotes the maximum angle of the tangent direction in cutting process (0=0°), and T_d denotes the period of the vertical stripes.

According to Eq. (1), if the rotation speed is less than 300 rpm, the wavelength of the waviness will be less than 33 mm and affect the PSD1 specification. In order to make the waviness away from the PSD1 evaluation range, the spindle rotation speed of 390 rpm is optimized as the work speed.

3.4 Machining process

During the machining process as shown in Fig. 11a, the cutter will leave tool marks on the machined surface; Fig. 11b shows the tool mark in ideal state; Fig. 11c shows the tool mark considering the error in z direction; Fig. 11d shows the tool mark considering the error in y direction. It can be found that

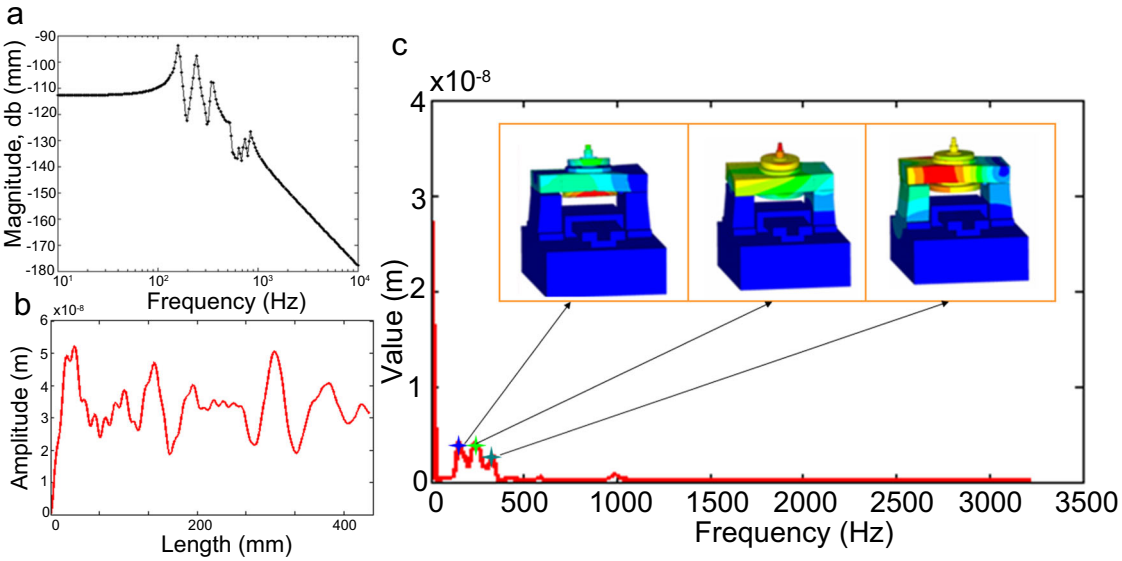

Fig. 10 Dynamic performance error of machine structure. **a** The dynamic performance of the machine tool, **b** the response of the machine tool under cutting force, **c** the frequency domain analysis

the motion error of the cutter will leave different tool marks in the machined surface.

Figure 12a shows the simulation surface considering the motion error of the tool cutter. The following parameters are used, cutting conditions: depth of cut of 15 μm, feed rate of 60 μm/s, and a spindle rotational speed of 390 r/min, and the tool parameters: tool nose radius of 5 mm, tool rake angle of −25°, and front clearance angle of 8°.

Figure 12b shows the PSD analysis of the simulation result; it can be found that the tool mark mainly gathered in 35.7 and 66.7 μm mainly affect the roughness specification.

3.5 Errors caused by environment vibration

Environment vibration spreads through soil around to the base of the machine or its located building, and eventually reaches the ultra-precision machine leading to the accuracy reduction. The vibration of the ground cause by the vehicle is the most important and common component of the environment vibration.

Nakamura et al. studied the ground slight vibration caused by the vehicle based on the power spectral density function of Kanai-Tajimi and given a correction formula as shown in Eq. 2, which is used to simulate acceleration power spectral density of ground motion caused by vehicle in this paper [21, 22].

$$S_{xx}(\omega)=\frac{\left[1+4\tau_{g1}^2\left(\frac{\omega}{\omega_{g1}}\right)^2\right]\left(\frac{\omega}{\omega_{g1}}\right)^2 s_0^2}{\left\{\left[1-\left(\frac{\omega}{\omega_{g1}}\right)^2\right]^2+4\tau_{g1}^2\left(\frac{\omega}{\omega_{g2}}\right)^2\right\}\left\{\left[1-\left(\frac{\omega}{\omega_{g1}}\right)^2\right]^2+4\tau_{g2}^2\left(\frac{\omega}{\omega_{g2}}\right)^2\right\}} \tag{2}$$

where $\omega_{g1},\tau_{g1},\omega_{g2},\tau_{g2}$ are the parameters of the ground motions, s_0 is the amplitude parameters of the PSD.

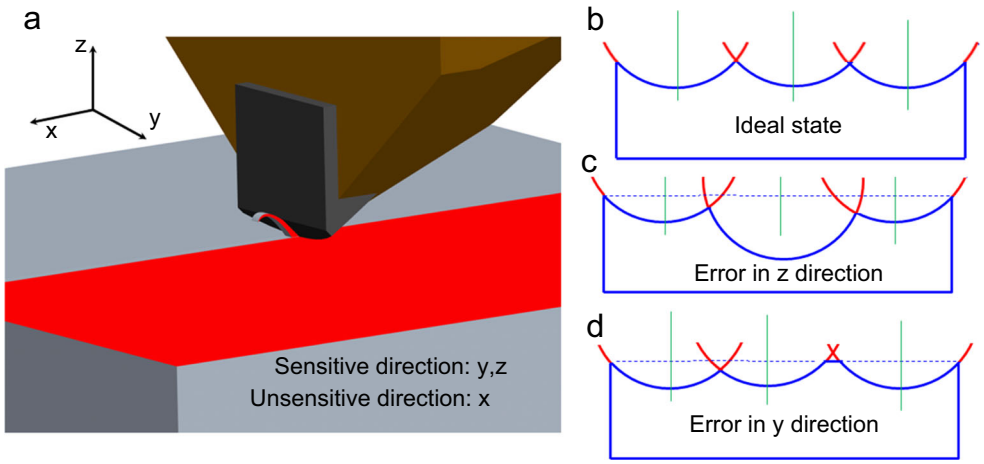

Fig. 11 Error in machining process. **a** Schematic diagram of machining process. **b** Ideal tool mark, **c** tool mark consider the error in z direction, **d** tool mark consider the error in y direction

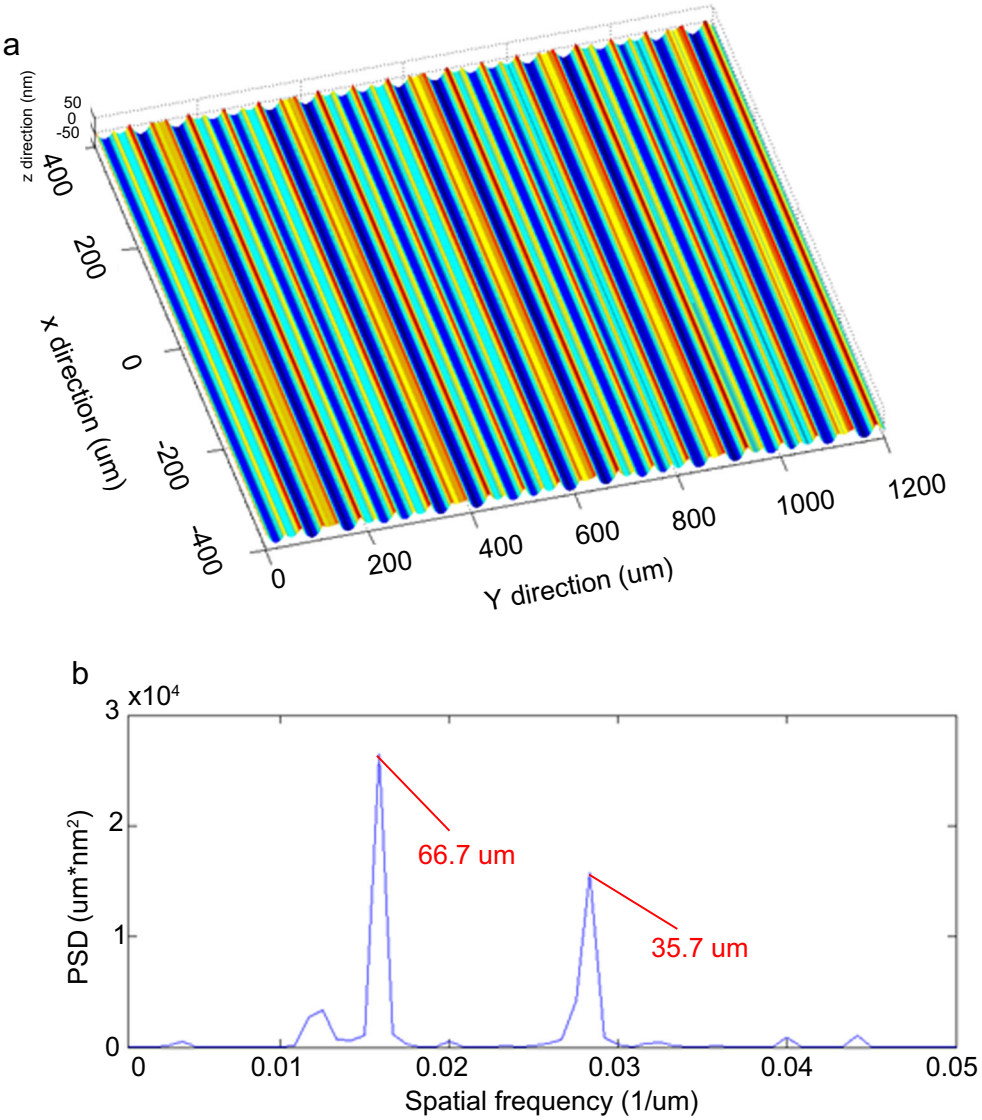

Fig. 12 Cutting mark simulation. **a** Simulation surface; **b** PSD analysis

The signal of the acceleration power spectral density of ground motion caused by vehicle is shown in Fig. 13a. It can be found that the frequency mainly in 10–30 Hz, then the signal is input to the FE model, and two output points in cutter and workpiece are obtained, respectively, as shown in Fig. 13b. Figure 13c shows the acceleration power spectral density and displacement of the cutter and workpiece; it shows that in the low-frequency range, the machine tool has the same acceleration power spectral density of the ground, and though the vibration of the ground is a low-frequency vibration, it can cause high-frequency vibration of the machine tool. In the high-frequency range, the influence of the ground vibration is more obvious on the cutter than the workpiece, which is because the amplitude of vibration is enlarged when passing to the machine tool through the bottom. Therefore, in order to ensure the accuracy of the machine tool, the isolation mounting is necessary.

4 Spatial frequency domain error budget

Figure 14 shows the error budget table; the main influence factor on each specification is listed; it not only help the designer to budget the spatial frequency error of the machine tool, but also indicate the direction to the designer by improving which performance of the machine tool can meet the requirement of a specified specification. It can be noted that the specification 1 mainly affects the mark of the cutter in the cutting process; the amplitude is 2 nm. The specification 2 mainly affect the pressure fluctuations of the oil source, the wavelength in 0.5–1.5 mm, the amplitude about 10 nm. The specification 3 mainly affect the dynamic performance, and this work presents an opportunity to optimize the rotation speed of the spindle from 300 to 390 rpm to minimize errors. The specifications 4 and 5

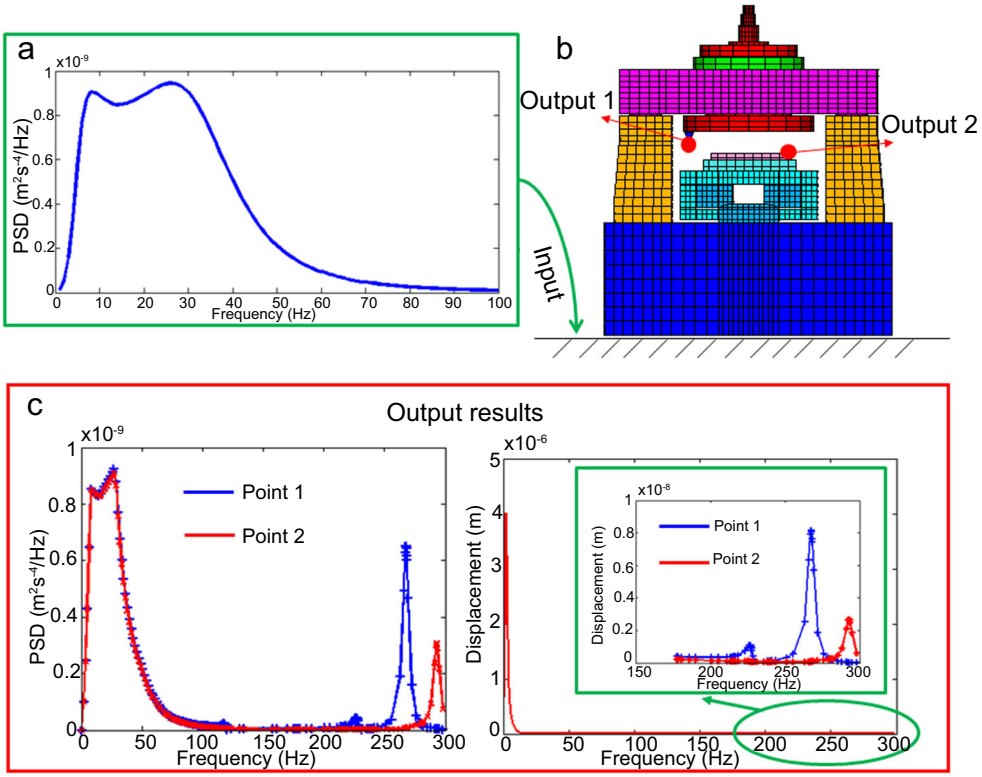

Fig. 13 The error analysis of the vibration of the ground cause by the vehicle

mainly affect the slide straightness and the spindle motion error. From the error budget table, it indicates that this flycutting machine tool can be used to product the KDP crystal.

5 Conclusion

The performance prediction and spatial frequency domain error budget method for designing and characterizing

Spatial Frequency Domain Error Budget

Axis	Feature	Units	Intrinsic	Abbe Error (m)	Roll Offset (m)	Max Error (um) X	Y	Z	Notes
X Axis	Pitch	Arc Sec	2	0.149		1.49			Quasi-static error
	Yaw	Arc Sec	2	0.083		0.83			Quasi-static error
	Roll Error in Y	Arc Sec	2		0.149		1.49		Quasi-static error
	Roll Error in Z	Arc Sec	2		0			0	Quasi-static error
	Straightness-Y	um	0.75				0.75		Quasi-static error
	Straightness-Z	um	0.75					0.75	Quasi-static error
	Positioning acc	um	1			1			Quasi-static error
Oil source		nm	spatial range: 0.5-1.5 mm					10	Oil source fluctuations
Spindle	Radial motion X		0.222			0.222			Quasi-static error
	Radial motion Y		0.222				0.222		Quasi-static error
	Axial motion Z		0.083					0.083	Quasi-static error
	Radial motion X	um	0.0908			0.0908			Dynamic error of 300 rpm
	Radial motion Y	um	0.0908	Frequency range: 0.98 and 6.5 Hz			0.0908		Dynamic error of 300 rpm
	Axial motion Z	um	0.0611					0.0611	Dynamic error of 300 rpm
Machine structure	Z-direction	um	Frequency range:170, 192, 336 Hz					0.04	Dynamic response in the machining process
Cutting process	Z-direction	nm	Spatial range:35.7 and 66.7					2	Mark of the cutter
					Static error(um)	3.542	2.553	0.843	
					Dynamic error	um		0.002	Spatia range 0.01-0.12mm
						nm		10	Spatia range 0.12-2.5mm
									Spatia range 2.5-33mm
						um		0.8511	Spatia range >33mm

Fig. 14 spatial frequency domain error budget table

machines used to manufacture or inspect parts with SFBS is presented, and this method is used to an ultraprecision flycutting machine tool for KDP crystal machining. In terms of the results and discussions presented, the main conclusions drawn are as follows:

1. The dynamic error budget method bridges the gap between the spatial frequency domain error prediction and the machine tool performance. It provides a better understanding of the further design of the performance of ultraprecision machines from spatial frequency domain.
2. The error in machining process is analyzed in spatial frequency domain, and the influence of each error on the machined results is discussed. The dynamic performance of the machine tool structure and the oil source fluctuations have significant effects on the SFBS.
3. This spatial frequency-based error budget encompasses the entire machine design as an entire system; the proposed design approach can be used as a powerful tool for supporting the full design process of machines used to manufacture or inspect parts with spatial frequency-based specifications.

Acknowledgments The authors gratefully acknowledge financial support of the Major Project of High-end CNC Machine Tool and Basic Manufacturing Equipment of China (2013ZX64006011-102-001).

References

1. Painsner JA, Boyes JD, Kuopen SA (1994) National ignition facility. Laser Focus World 30:75
2. Lin ZQ (1999) SG-II laser elementary research and precision SG-II program. Fusion Eng Des 44:61–66
3. Shore P, Morantz P, Luo X, Tonnellier X, Collins R, Roberts A, Miller R, Read R (2005) Large optix ultra-precision grinding/measuring system. Proceedings of SPIE-The International Society for Optical Engineering Q:1–8.
4. Li MQ, Chen MJ, Cheng J, Xiao Y, Jiang W (2013) Two important mechanisms damaging KH_4PO_2 crystal processed by ultraprecision fly cutting and their relationships with cutting parameters. Appl Opt 52:3451–3460
5. Chen MJ, Li MQ, Cheng J, Jiang W, Wang J, Xu Q (2011) Study on characteristic parameters influencing laser-induced damage threshold of KH_2PO_4 crystal surface machined by single point diamond turning. J Appl Phys 110:113103
6. Donaldson RR (1972) A simple method for separating spindle error from test ball roundness error. Ann CIRP 21:125–126
7. Slocum AH. in: Precision Machine Design, Englewood Cliffs, Prentice Hall, 1992.
8. Treib T, Matthias E (1987) Error budgeting—applied to the calculation and optimization of the volumetric error field of multiaxis systems. CIRP Ann Manuf Technol 36:365–368
9. Error budget as a design tool for ultra-precision diamond turning machines, http://ebookbrowsee.net/1023-pdf-d32511414
10. Johan G (1995) Error budgeting for control system design. RD J 11: 61–67
11. Hii KF, Zhao XH, Vallance RR (2000) Design of a precision electro discharge micro milling machine. Proceedings of the American Society of Precision Engineers Annual Conference. Scottsdale, Arizona. October 22–27.
12. Krulewich D, Hauschildt H (1998) Spatial frequency domain error budget, 13th Annual Meeting of the American Society for Precision Engineering, St. Louis, MO, October 25–30.
13. Lahaye P, Chomont C, Dumont P, Duchesne J, Chabassier G (1999) Using a design of experiment method to improve KDP crystal machining process. SPIE 3492:814–820
14. Spaeth ML, Manes KR, Widmayer CC (2004) National ignition facility wavefront requirements and optical architecture. Opt Eng 43:2854–2865
15. Aikens D (1995) Derivation of preliminary specifications for transmitted wavefront and surface roughness for large optics used in Inertial Confinement Fusion. Proc SPIE 2633:350–360
16. Chen WQ, Liang YC, Sun YZ, An CH, Chen GD (2014) Investigation of the influence of constant pressure oil source fluctuations on ultra-precision machining, Proc IMechE Part B: J Engineering Manufacture, doi:10.1177/0954405414530694
17. Liang YC, Chen WQ, An CH, Luo XC, Chen GD, Zhang Q (2014) Investigation of the tool-tip vibration and its influence upon surface generation in flycutting, Proc IMechE Part C:J Mechanical Engineering Science doi:10.1177/0954406213516440
18. Sun YZ, Chen WQ, Liang YC, An CH, Chen GD, Su H (2014) An integrated method for waviness simulation on large-size surface, Proc IMechE Part B: J Engineering Manufacture doi:10.1177/0954405414525143
19. Chen WQ, Liang YC, Sun YZ, Huo DH, Lu LH, Liu HT (2014) Design philosophy of an ultra-precision fly cutting machine tool for KDP crystal machining and its implementation on the structure design. Int J Adv Manuf Technol 70: 429–438
20. Liang YC, Chen WQ, Bai QS, Sun YZ, Chen GD, Zhang Q, Sun Y (2013) Design and dynamic optimization of an ultraprecision diamond flycutting machine tool for large KDP crystal machining. Int J Adv Manuf Technol 69:237–244
21. Kanai K (1957) Semi-empirical formula for the seismic characteristics of the ground. Tokyo Univ Earthq Res Inst Bull 35: 307–325
22. Yang ZC, Xu YL (2003) Studies on the integrated active control of micro vibration for Hi-Tech facilities. J Northwest Polytech Univ 21(6):646–649